Available online at www.sciencedirect.com

ScienceDirect

Procedia Structural Integrity 7 (2017) 275–282

Structural Integrity Procedia

www.elsevier.com/locate/procedia

3rd International Symposium on Fatigue Design and Material Defects, FDMD 2017, 19-22 September 2017, Lecco, Italy

Quality control of cast iron: extreme value statistics applied to CT measurements

S. Romano[a,*], S. Beretta[a], M. Cova[b]

[a] *Politecnico di Milano, Dipartimento di Meccanica, Via La Masa 1, I 20156 Milano*
[b] *SACMI Imola S.C., Via Selice Provinciale 17/A, I 40026 Imola (BO)*

Abstract

In this presentation, we will summarize the main results of a research activity aiming at predicting the size of the defect at the origin of fatigue failure in large spheroidal cast iron presses. The endurance limit of the material is largely influenced by the ineluctable presence of defects related to the casting process, such as voids and degenerated graphite. The aim of this activity was to determine a reliable and robust way to control the material in production and to reject the parts which do not meet the company's quality requirements. Defect measurements have been performed with 2D and 3D techniques (i.e. metallographic analyses and computed tomography) and different maxima sampling strategies have been applied to the data, to determine a reliable and robust distribution of the largest defects. The maximum defect in the component volume was estimated adopting the concepts of statistics of extremes. The goodness of the results has finally been validated considering the largest defect detected in the most stressed component volume.

Peer-review under responsibility of the Scientific Committee of the 3rd International Symposium on Fatigue Design and Material Defects.

Keywords: defect tolerant fatigue assessment; computed tomography; statistics of extremes; spheroidal cast iron; degenerate graphite

Nomenclature

A	area
BM	Block Maxima sampling
CT	computed tomography
F	cumulative probability
MA	metallography
n	volume ratio for the application of statistics of extremes

* Corresponding author. Tel.: +39-02-2399-8248; fax: +39-02-2399-8263.
E-mail address: simone.romano@polimi.it

Peer-review under responsibility of the Scientific Committee of the 3rd International Symposium on Fatigue Design and Material Defects.
10.1016/j.prostr.2017.11.089

N_u	number of exceedances over the threshold
POT	Peaks-over threshold
u	threshold for POT maxima sampling
V	volume
V_0	control volume for maxima sampling
V_c	component reference volume
V_n	volume to be considered applying statics of extremes
V_{ref}	reference volume for data comparison
λ, δ	scale and shape parameters of the Gumbel distribution
ρ_u	density of exceedances over the threshold
σ	parameter of the negative exponential distribution

1. Introduction

How to deal with fatigue in presence of defects is an old and deeply investigated topic. After the introduction of defect tolerant design concepts in the mid 1980s by Murakami and Endo (1986), this kind of analysis has been adopted for several applications and various materials and manufacturing techniques. The application of these concepts requires the estimation of the maximum defect which can occur inside a component. Sometimes, this information is not available a-priori, therefore quantitative measurements together with specialised statistical analyses are required. This is the case of the presses analysed in this paper. Given their massive dimension, the small production numbers and the different contractors providing the cast raw parts, the quality of the castings may be variable and heterogeneous. Due to the cost of discarding the raw parts, the company wants to improve the quality assessment and acceptability rules and define an internal procedure to be applied on all the parts before starting the following manufacturing phase.

1.1. Scope on detection and analysis of extreme defects

The dangerous defect types that can be found in the cast iron are porosity and degenerate graphite. An easy and cheap way to measure the defect distribution is the investigation of small polished sections at the microscope, which was often used in the past due to the lack of more sophisticated techniques (see Murakami (1994)). When the defects become the fracture origin, it is well recognized that, in a volume of material subjected to the same cyclic stress, the fatigue failure occurs at the largest defect or inhomogeneity (see Murakami (2002)). Therefore, the estimation of fatigue strength in presence of defects needs the estimate of the prospective size of maximum defect in the component volume. The impossibility to prepare and analyse large material areas was overcome adopting the concepts of statistics of extremes (see Coles (2001); Reiss and Thomas (1997)), which allows to estimate the distribution of the maximum defect in a larger volume of material than the one investigated.

Needing only the dimension of the maximum defects, the *block maxima* (BM) sampling can be used. This sampling strategy consists in subdividing the area in several sub-parts and measuring only the largest defect detected in each one. The size of the defects is usually expressed considering the $\sqrt{area}$ parameter. The resulting data can then be described by a Gumbel distribution (Murakami and Beretta (1999) provides a summary of this research). Although it is commonly used and described in the standard `ASTM E2283-03` (2003), this process has some drawbacks (e.g. bi-dimensional measure, small sampling areas achievable, need to polish the surface, definition of the reference area for the BM application not straightforward). Moreover, the measurements obtained from 2D analyses do not refer to the maximum size of the defect, but the position in which the polished section intersects them is random. Therefore, a general underestimation of the maximum defect size can generally be expected. This limitation can be overcome applying probabilistic coefficients dependent on the shape of the defects (see Sahagian and Proussevitch (1998)), but the application of these concepts can become very inaccurate when dealing with complex shapes as in the present case.

A more actual and simple way to measure the defects is the adoption of computed tomography (CT). Even being more expensive, this technique allows to analyse large material volumes and has the further advantage of describing

the defect population in 3D without needing any surface preparation. For these reasons, the adoption of CT for the defect description is quickly increasing in the last years, especially for cast (see for example Shirani and Härkegård (2012); Wicke et al. (2016)) and additive manufactured (see Thompson et al. (2016) for a review) parts. Romano et al. (2017) showed the application of statistics of extremes to CT scan data to give a proper description of the maximum defects in aluminium samples produced by additive manufacturing. Moreover, the adoption of a *peaks-over threshold* (POT) maxima sampling was seen to provide the same results of BM with a more rapid and simple data processing. This sampling method consists in saving all the measurements larger than a given threshold u, whose determination is simpler than the reference area to apply for BM (see Beretta et al. (2006)). In this way, one can be sure that no important data are lost.

In the following, the data obtained on polished sections and CT will be presented and analysed by both sampling methods introduced and the estimates obtained by statistics of extremes will be used to define a quality index for the material.

2. Material and experiments

The material investigated is spheroidal cast iron, *EN-GJS-400-18-U*. Four cast parts with low quality have been investigated, from now on numbered from 1 to 4. A scheme of the component is depicted in Fig. 1b. The most stressed zone of the press is the one close to the pre-filling hole. The critical component volume $V_c = 2.4 \cdot 10^6$ mm^3 has been calculated by finite element analysis as the volume subjected to a stress exceeding the 90% of the maximum one. As the defect formation is strictly linked to the cooling rate during the casting process, the part is heterogeneous and anisotropic. Therefore, the material investigated was extracted close to the critical region, as depicted in Fig. 1b.

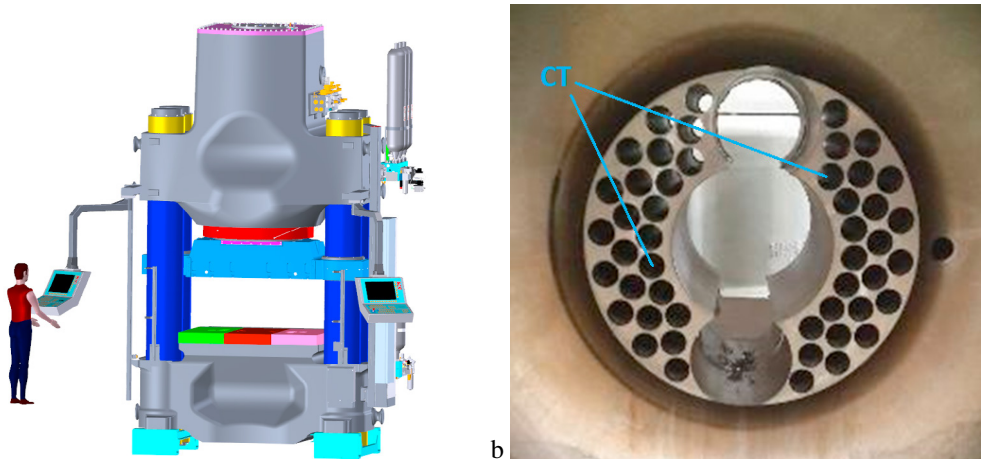

Fig. 1. Component and material investigated: (a) scheme of the press; (b) upper crossbeam after coring and position of the samples investigated by CT.

The specimens extracted have a cylindrical shape, with a diameter equal to 15 mm or 18 mm and a length of 60 mm or 100 mm. Tab. 1 reports the number of specimens N and the quantity of material investigated by MA and micro CT. In order to compare the results of 2D and 3D techniques, an empirical rule by Uemura and Murakami (1990) has been adopted to calculate an equivalent observed volume V_{MA} from bi-dimensional analyses. This volume can be defined according to Eq. 1, where A_{MA} is the area investigated and h is the average dimension of the maximum defects detected by BM in terms of $\sqrt{area}$.

$$V_{MA} = A_{MA} \cdot h \tag{1}$$

As the CT results are directly related to the density of the material crossed by the X-rays, it is sometimes possible to distinguish between different defect types by accurately selecting the grey scale of interest. This kind of analysis has been developed by SACMI by a proprietary semi-automatic procedure able to identify the presence of degenerate

Table 1. Summary of the material investigated.

Material	N_{MA}	A_{MA} (mm^2)	V_{MA} (mm^3)	N_{CT}	V_{CT} (mm^3)
1	6	$2.5 \cdot 10^3$	$3.1 \cdot 10^3$	3	$4.9 \cdot 10^4$
2	6	$2.5 \cdot 10^3$	$2.5 \cdot 10^3$	1	$1.5 \cdot 10^4$
3	12	$5.2 \cdot 10^3$	$7.7 \cdot 10^3$	2	$2.4 \cdot 10^4$
4	12	$5.0 \cdot 10^3$	$3.6 \cdot 10^3$	2	$2.7 \cdot 10^4$

graphite and distinguish it from the voids. After the reconstruction, it is possible to export the size, shape and position of all the voids and degenerate graphite, considered separately or together.

3. Results

The main results obtained by CT scan are here summarized. The main steps of the analysis are exemplified considering material 1. Fig. 2a shows the defect distributions measured in the two samples investigated, considering the voids and degenerate graphite as two distinguished defect types. Defect density is in some cases inhomogeneous as in Fig. 2b, due to the cooling rate gradient after the casting process.

In all the samples investigated, the number and size of voids are smaller than those of the degenerate graphite. This confirms the experimental evidence that the degenerate graphite is the most detrimental defect type for this components. However, some voids can sometimes be detected close to degenerate graphite regions (see an example in Fig. 2c), reason why the data considered in the following refers to measurements performed without making any defect type distinction.

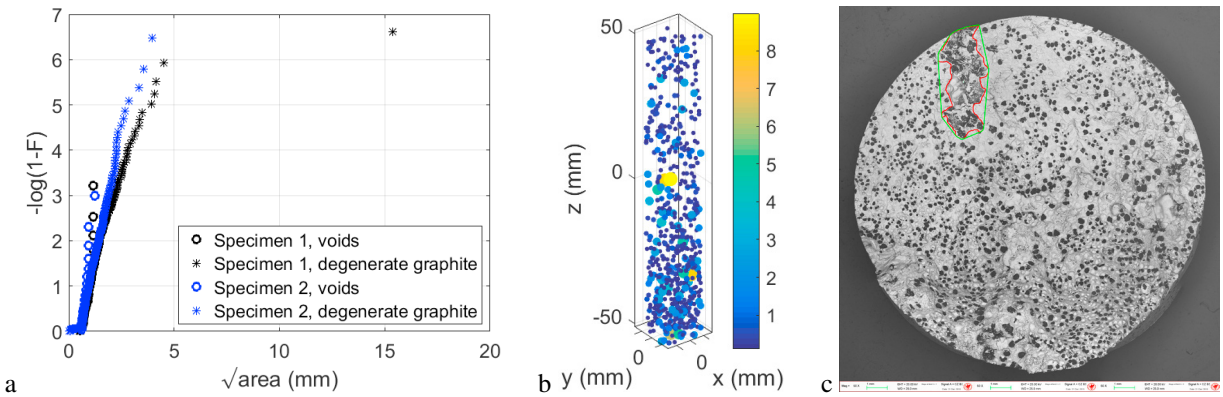

Fig. 2. Defects inside material 1: (a) defect distribution for voids and porosity in a negative exponential probability plot; (b) defect position in specimen 1; (c) fracture surface of a fatigue specimen showing the defect at the origin of failure.

Being a 3D technique, CT also allows to detect possible defect elongation directions. In some specimens some differences in the $\sqrt{area}$ projected along the three principal directions highlighted a preferential direction for elongation. In order to obtain a conservative assessment, the direction associate with the largest dimensions was considered.

3.1. Maxima sampling strategies

A block maxima sampling was applied on all the data detected by MA and CT. In the first case, the maximum defect detected in every area investigated was selected, as depicted in Fig. 3a. Considering CT, instead, the specimens were divided into eight equivalent subvolumes. In order to reduce the influence of the defect density gradient, the subvolumes were obtained cutting with planes parallel to the axis of the sample, as shown in Fig. 3b.

POT has been applied following the path described by Romano et al. (2017). All the data show a change of slope at a size close to the maximum measured void. This happens because the first part of the curve contains both defect

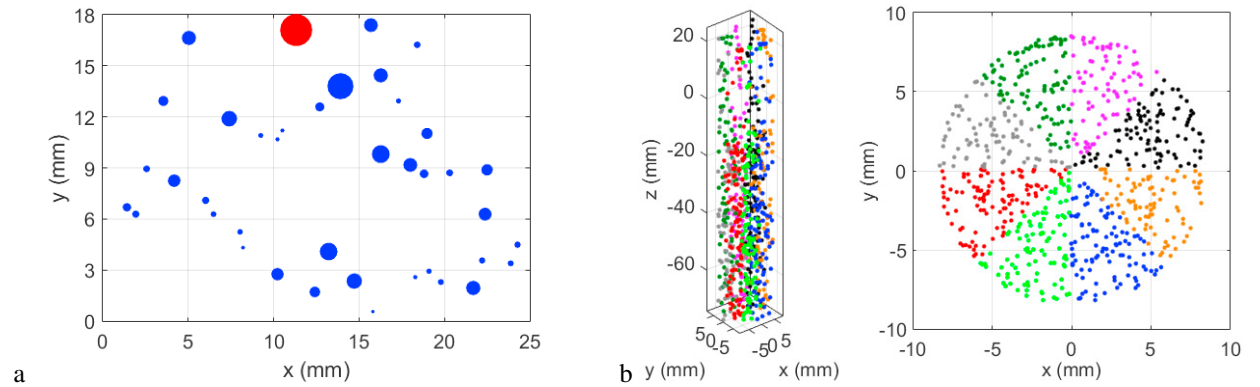

Fig. 3. Application of BM sampling: (a) maximum defect detected by metallography in a sample area; (b) volume subdivision applied to material 1, sample 1.

types, while the second one concerns only the degenerate graphite. Defining a threshold after this knee point allows to model the large data with a unique parameter and to focus only on the most detrimental defect type. The parameter σ of the negative exponential distribution is easily calculated as the average size of the exceedances. In order correctly model the data, all the exceedances must align in the exponential probability plot and fall inside the confidence band. The threshold adopted and the parameters of the distributions obtained for the four materials are summarized in Tab. 2, while Fig. 4 shows the application of the method to material 1.

Table 2. Parameters of the negative exponential maximum defect distribution after POT.

Material	u (mm)	N_u	ρ_u (def/mm^3)	σ (mm)
1	1.5	120	$4.0 \cdot 10^{-3}$	0.708
2	1.0	10	$6.7 \cdot 10^{-3}$	0.442
3	1.25	11	$3.6 \cdot 10^{-4}$	0.980
4	1.25	10	$6.5 \cdot 10^{-4}$	0.925

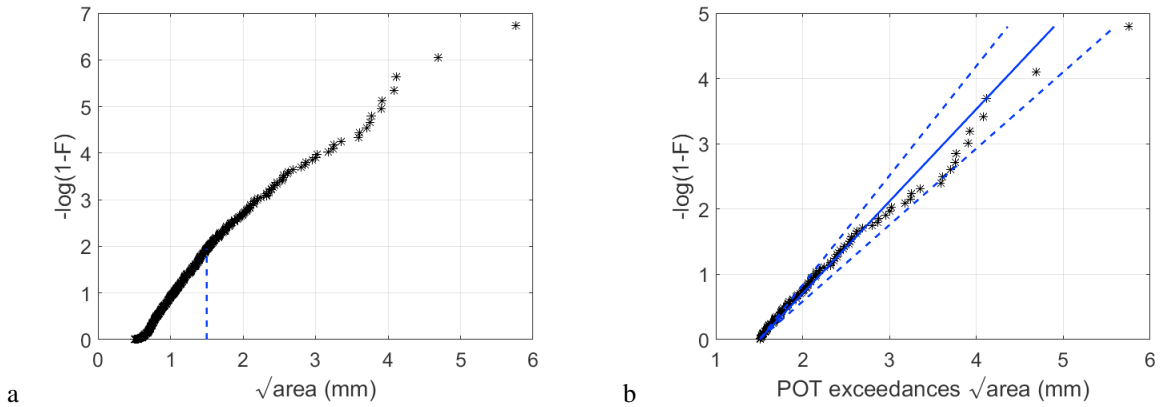

Fig. 4. Application of POT maxima sampling: (a) change of slope over u = 1.5 mm; (b) negative exponential distribution of the exceedances and 95% confidence band.

3.2. Application of statistics of extremes

The maxima obtained by BM in the sampling volume V_0 have been described by a Gumbel distribution, defining the scale parameter λ and a shape parameter δ. The Gumbel distribution is the most used, simple and robust way to describe extreme events (Murakami and Beretta (1999)). The same can be done considering POT maxima sampling, as the negative exponential distribution becomes equivalent to a Gumbel when the data are far larger than the threshold. Under this hypothesis, the Gumbel's parameters can directly be derived from those of the exponential distribution, applying Eq. 2.

$$\begin{cases} \delta = \sigma \\ \lambda = u + \sigma \cdot \log(N_u) \end{cases} \tag{2}$$

V_0 can be determined as the total volume investigated divided for the number of maxima selected, which have been reported in section 3.1. These volumes are $V_{0,MA} = V_{MA}/N_{MA}$ and $V_{0,CT} = V_{CT}/8$ for BM sampling and $V_{0,CT,u} = V_{CT}/N_u$ for POT. One interesting property of the Gumbel distribution is that, when statistics of extremes is applied, the resulting distribution is still a Gumbel having the same shape parameter. The scale parameter, instead, increases with the volume ratio $n = V_n/V_0$, according to Eq. 3.

$$\begin{cases} \delta_n = \delta \\ \lambda_n = \lambda \cdot \ln(V_n/V_0) \end{cases} \tag{3}$$

The larger the sampling volume, the larger the dimension of the maximum defect, therefore the results obtained by MA and CT are not directly comparable. In order to compare the results, all the distributions must refer to the same volume of material. This was achieved applying Eq. 3 to the different maxima samplings performed to refer to the same reference volume V_{ref}, which was arbitrarily set to 1000 mm^3. The estimates obtained for material 1 are depicted in the Gumbel probability plot of Fig. 5. The goodness of the estimated distribution can be verified looking at the position of maximum defect detected in the component reference volume, which has an ordinate equal to $\log(V_c/V_{ref})$. Fig. 5a shows that MA gives non-conservative estimates of the maximum defect in the most stressed volume. A far better results was achieved applying BM on CT data, even if the confidence of the result is relatively low. For all the four materials, the most robust and accurate option was seen to be the adoption of POT on CT data, depicted in Fig. 5b.

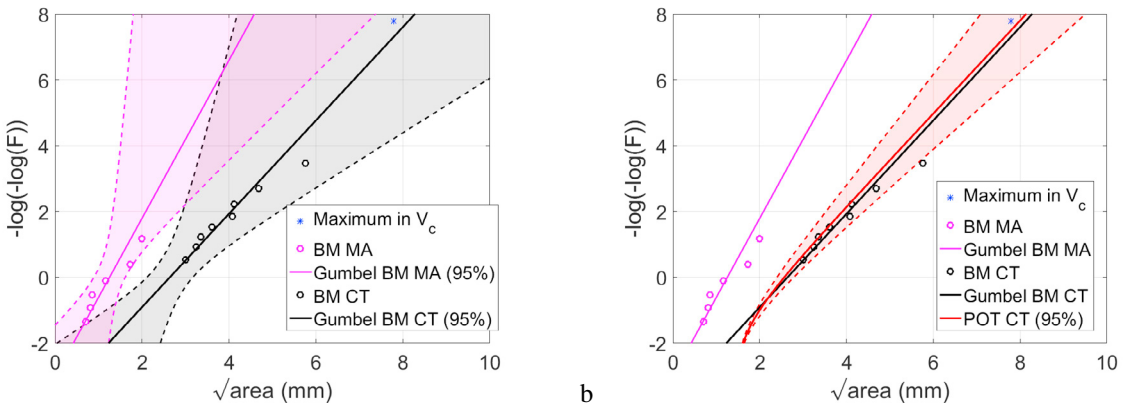

Fig. 5. Distribution of the maximum defect obtained with the three methods proposed and maximum defect found in V_c: (a) BM on MA and CT data; (b) POT on CT data.

A clear visualization of the expected size of the maximum defect can be obtained plotting the maximum defect distribution estimated with POT on CT data as a function of the volume analysed with statistics of extremes, as in Fig. 6. In all the cases, the distribution is able to give a good estimate of both the maxima obtained by BM on CT data and the maximum defect detected in the whole component 90% volume V_c.

Finally, Tab. 3 summarizes the estimated maximum defect size and the experimental measurement in V_c. In all cases, the maximum defect detected in the component falls inside the 95% scatter band.

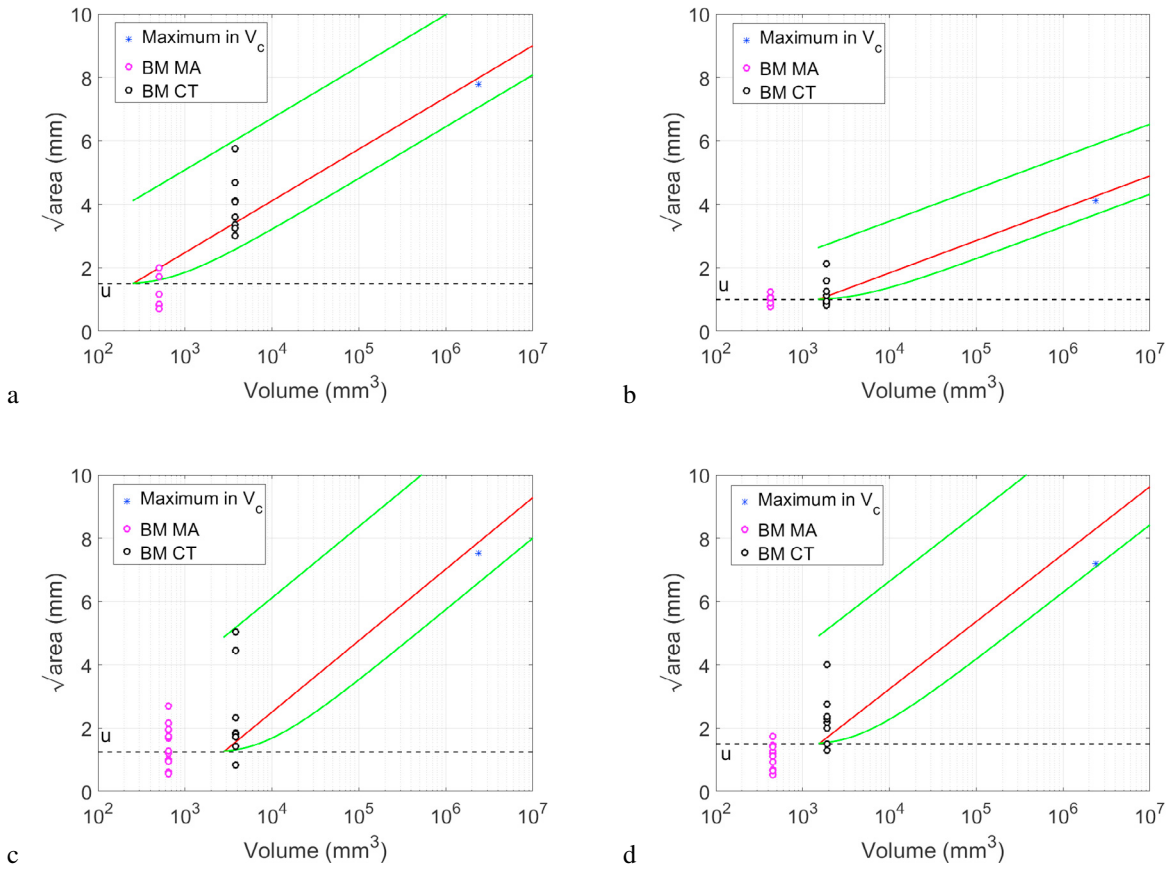

Fig. 6. Statistics of extremes estimates for different material volumes with 95% scatter band (green) and characteristic maximum (red) for: (a) material 1; (b) material 2; (c) material 3; (d) material 4.

Table 3. Maximum defect size estimated compared to the maximum measurement in V_c.

Material	Max. experimental (mm)	Maximum characteristic estimate (mm)	2.5% percentile (mm)	97.5% percentile (mm)
1	7.8	8.0	7 1	8.9
2	4.1	4.3	3.7	4.9
3	7.5	7.9	6.6	11.4
4	7.2	6.9	6.0	7.8

4. Discussion

In all the materials analysed, the presence of voids could always be considered irrelevant with respect to degenerate graphite, except in the cases in which both the defect types were detected in the same regions. In general, different behaviours could be expected considering materials showing a better overall quality, reason why considering both the defect types in the same analysis gives a more robust result.

Peaks-over threshold maxima sampling was seen to ensure the best performance. The choice of the threshold can slightly influence the results, but a unique value can be used for all the materials, equal to 1.25 mm. Note that the application of POT does not allow to make estimates for a defect size lower than u. Some anisotropy and heterogeneity of the material and of defect elongation have been detected in different samples and even inside the same one. The three dimensional measurements obtained by computed tomography allow obtaining a more precise characterization

and more robust assessments than MA. Moreover, in Fig. 6 it can be seen that in most cases the maxima detected with MA analyses are below the threshold. This means that these points are describing the first slope of the data shown in Fig. 4, reason why the estimates result lower than the real experimental values. Better results can be obtained analysing larger areas of material, but the experimental effort required to obtain robust estimates can be too high for a standard control in production.

The maximum defect detected in the component volume fell in all cases inside the 95% scatter band, thus validating the application of statistics of extremes. The method proposed was able to correctly estimate a defect size ranging between 4 mm and 8 mm. Knowing the critical defect size, the quality analysis can be based on the assessment of a safe percentile of the maximum defect distribution related to the volume V_c.

5. Conclusions

In this paper, a method to define the quality of spheroidal cast iron containing manufacturing defects has been implemented, in order to define an acceptance criterion. Statistics of extremes was applied to metallographic and tomographic measurements, analysed with different maxima sampling methods. The significant results of the activity can be so summarized:

- the analyses of metallography do not give acceptable results, resulting in a repeated underestimation of the maximum defect size;
- the adoption of CT allows to obtain better results because of the larger volume analysed. At the same time, a 3D measure of defect shape and position gives a better understanding of the real anisotropy and heterogeneity;
- the significant defects can be selected among the measurements applying a maxima sampling strategy. The application of POT yields better precision and confidence with respect to BM sampling;
- statistics of extremes applied to CT data was in all cases able to estimate the maximum defect size in the most stressed component volume. Material quality can therefore be assessed defining the maximum defect expected in the reference component volume.

References

ASTM E2283-03, 2003. Standard practice for Extreme Value Analysis of Nonmetallic Inclusions in Steels and Other Microstructural Features. American Society for Testing And Materials.

Beretta, S., Anderson, C., Murakami, Y., 2006. Extreme Value Models for the Assessment of Steels Containing Multiple Types of Inclusion. Acta Materialia 5, 2277–2289.

Coles, S., 2001. An Introduction to Statistical Modeling of Extreme Values. Springer, London.

Murakami, Y., 1994. Inclusion rating by statistics of extreme values and its application to fatigue strength prediction and quality control of materials. J. Res. Natl. Inst. Stand. Tehcnol. 99, 345–351.

Murakami, Y., 2002. Metal Fatigue: Effects of Small Defects and Nonmetallic Inclusions. Elsevier, Oxford.

Murakami, Y., Beretta, S., 1999. Small Defects and Inhomogeneities in Fatigue Strength: Experiments, Models and Statistical Implications. Extremes 2, 123–147. doi:10.1023/A:1009976418553.

Murakami, Y., Endo, M., 1986. Effect of hardness and crack geometries on $\Delta K_t h$ of small cracks emanating from small defects, in: Miller, K., Rios, E.D.L. (Eds.), The Behaviour of Short Fatigue Cracks. MEP.

Reiss, R., Thomas, M., 1997. Statistical Analysis of Extreme Values. Birkhauser Verlag, Basel.

Romano, S., Brandão, A., Gumpinger, J., Gschweitl, M., Beretta, S., 2017. Qualification of AM parts: extreme value statistics applied to tomographic measurements. Materials & Design , 1–34.

Sahagian, D.L., Proussevitch, A.A., 1998. 3D particle size distributions from 2D observations: stereology for natural applications. Journal of Volcanology and Geothermal Research , 173–196.

Shirani, M., Härkegård, G., 2012. Damage tolerant design of cast components based on defects detected by 3d x-ray computed tomography. International Journal of Fatigue 41, 188–198.

Thompson, A., Maskery, I., Leach, R.K., 2016. X-ray computed tomography for additive manufacturing: a review. Meas. Sci. Technol. 27, 072001. doi:http://dx.doi.org/10.1088/0957-0233/27/7/072001.

Uemura, Y., Murakami, Y., 1990. A Numerical Simulation of Evaluating the Maximum Size of Inclusions to Examine the Validity of the Metallographic Determination of the Maximum Size of Inclusions. Trans. Japan Soc. Mech. Eng. Ser. A 56, 162–167.

Wicke, M., Luetje, M., Bacaicoa, I., Brueckner-Foit, A., 2016. Characterization of Casting Pores in Fe-rich Al-Si-Cu Alloys by Microtomography and Finite Element Analysis. Procedia Structural Integrity 2, 2643–2649. doi:10.1016/j.prostr.2016.06.330.